International Journal of Applied Mathematics

Volume 38 No. 8s, 2025

ISSN: 1311-1728 (printed version); ISSN: 1314-8060 (on-line version)

HARMONIC MITIGATION AND POWER FACTOR IMPROVEMENT IN GRID-TIED PV SYSTEMS USING INTELLIGENT CONTROL STRATEGIES

Soukaina Essaghir[1*], Tajeddine Khalili[2], Mustapha Oulcaid[1]

[1] Sultan Moulay Slimane University, Nationale School of Applied Sciences, ENSA – Beni-Mellal, LGS Laboratory,

Beni-Mellal, Morocco.

[2] Sultan Moulay Slimane University,

Nationale School of Applied Sciences, ENSA – Beni-Mellal, LICPM Laboratory,

Beni-Mellal, Morocco.

Abstract

This paper proposes an intelligent control strategy to improve the power quality in grid-connected photovoltaic (PV) systems. Conventional controllers such as proportional-integral (PI) and proportional-resonant (PR) controllers are studied and compared with intelligent counterparts, specifically fuzzy logic control (FLC) and fuzzy logic control optimized using Particle Swarm Optimization (FLC-PSO). The PV system with power electronic converters is modeled and simulated in MATLAB/Simulink under nonlinear load and different test conditions. Results show that the intelligent controllers significantly outperform the conventional control algorithms: FLC-PSO yields a total harmonic distortion (THD) of 4.7% while PI control achieves 36.1%; the power factor simultaneously increases from 0.86 (PI) to 0.99 (FLC-PSO). From the study it is proved that optimized fuzzy logic control not only reduces harmonics but also improves the grid compliance and energy conversion efficiency. These findings provide useful guideline for designing and implementing high-performance control strategies in modern PV systems, highlighting the practical potential of simulation-driven analysis for PV system integration.

Math. Subject Classification:

Keywords and Phrases: PV System, Grid, PR Controller, Fuzzy Logic Controller, PSO, TDD, PF, Non Linear Load.

1. Introduction

With the growing adoption of renewable energy sources, photovoltaic (PV) systems have become a key component for addressing global energy challenges [1], [2], [3], [4]. However, integrating PV systems into an electric grid presents several power quality issues, particularly in the presence of nonlinear loads and under variable solar-irradiance conditions. Such disturbances, including harmonic distortions and poor power factor, can affect grid stability and reduce the overall efficiency of power transmission [5], [6], [7].

Received: August 06 2025

In recent research, the performance of intelligent control strategies in dealing with challenges has been noted. Indicatively, study [8] has demonstrated that the proposed control (PSO+IC) and (PSO+PO) result in the better efficiency in the given system, decreasing the settling time, and the ripple output power. Besides, the analysis discussed in paper [9], suggests PSO algorithm implementation on maximizing both voltage stability and the overall performance of three-phase ship PV system by optimizing LCL parameters and LCL-GCI through CRNN-LM-BP control. Furthermore, investigation in [10] demonstrates that PSO finds extensive application in maximum power point tracking of photovoltaic power system, and it proves a high performance of hybrid PSO-FLC compared to PSO regarding to accuracy, efficiency and harmonic mitigation. Moreover, in our previous study [11], we evaluated the performance of three control strategies—Proportional-Integral corrector (PI), Proportional-Resonant regulator (PR), and Fuzzy Logic Control (FLC)—in a grid-connected PV system supplying a nonlinear load [12], this analysis demonstrated the superior harmonic mitigation capabilities and resilience of the fuzzy logic controller.

Despite these developments, the majority of the proposed studies apply this intelligent algorithm only in the MPPT control, or are limited to a PV system not connected to the grid, while the real disturbances are more significant when the PV system is connected to the grid and especially when it supplies a non-linear load and undergoes sudden variations in climatic conditions. To fill this gap, this paper evaluates the effectiveness of these controllers, proposes a robust **optimization of the FLC using the Particle Swarm Optimization (PSO) algorithm** on inverter controller, stresses an advanced analysis of some critical parameters like THD, TDD, PF and, primarily, the behavior of the studied system under the full change of climatic conditions or power supplies of non-linear loads.

To comprehensively evaluate the proposed control framework, this paper also:

- Investigates the **transient performance** of the control strategies under **variable irradiance and temperature conditions**, which reflect real-world PV system operation.
- Introduces additional **power quality indicators**, such as **Total Demand Distortion (TDD)** and **power factor**, to provide a more comprehensive assessment of system behavior.
- Benchmarks the performance of the PSO-optimized FLC against conventional PI, PR, and standard FLC approaches.

This proposed control is validated on the basis of MATLAB/Simulink simulation, it offers a more realistic and insightful analysis of PV system behavior under environmental and load-induced disturbances, it contributes to the advancement of power quality management, reducing harmonics, and enhancing power factor, which are critical for grid integration.

The research structure of this article is organized as follow: an overview of the studied system is introduced in section 2. Section 3 focuses on the control strategies for the current loops, covering PI, PR, and Fuzzy PI controllers. The next section describes the robust algorithm developed using the particle swarm optimization. Section 5 analyzes the measurement data as well as the inputs of the operations, followed by conclusion and finding keys in the final part.

Received: August 06 2025

Volume 38 No. 8s, 2025

ISSN: 1311-1728 (printed version); ISSN: 1314-8060 (on-line version)

2. Configuration and Modeling System

The system being studied is composed of a photovoltaic (PV) source attached to the power supply, which sends energy to a nonlinear load using successive power electronic converters and undulating control schemes. The analysis was performed using MATLAB/Simulink to simulate the setup and check its output against stable and variable environmental conditions. Figure 1 illustrates the topology of the modeled system based primary on a PV array, irradiance (G) and temperature (T) are varied to simulate real-life functioning conditions and determine their influences on the current output of the system. In order to see that the PV array is operating at the same time at the maximum power point, a boost converter is embodied so that the DC link voltage is controlled. The Perturb and Observe (P&O) algorithm [13], is one of the most common methods of Maximum Power Point Tracking (MPPT) applied in converter's controlling. The duty cycle of this algorithm is adjusted to optimize energy capture on real-time changes of the output power. After the voltage is controlled, the DC power converted is ready to be transformed to AC through a three-phase Voltage Source Inverter (VSI) [14]. Pulse Width Modulation (PWM) is used in the inverter to generate the required alternating switch signals whereby switching signals enable the connected output current to adjust to a desired reference signal (near sinusoidal) of low harmonic distortion, producing a high level of grid energy delivery efficiency [15], [16].

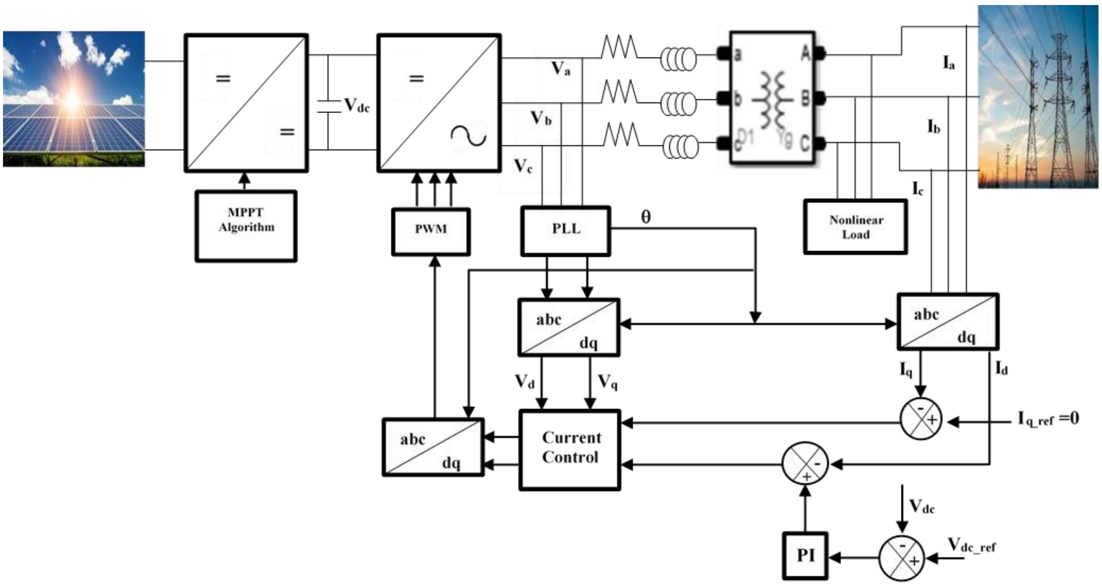

Figure 1. Topology of the modelled system

3. Current Control Strategy

Current control is a fundamental aspect of grid-connected inverter operation, ensuring stable and accurate power injection into the grid. The control strategy typically operates in the synchronous rotating reference frame (d-q frame), which streamlines the regulation of three-phase AC quantities by transforming them into DC-link components. This transformation is achieved using Clarke and Park transforms, allowing independent control of active and reactive power. To synchronize the inverter with the grid, a Phase-Locked Loop (PLL) [17] is employed, aligning the control signals with the grid voltage phase and frequency. Various

Received: August 06 2025

Volume 38 No. 8s, 2025
ISSN: 1311-1728 (printed version); ISSN: 1314-8060 (on-line version)

controllers such as Proportional-Integral (PI), Proportional-Resonant (PR), and Fuzzy Logic Controllers (FLC) can be implemented to manage the current in the d-q frame, each offering distinct advantages in terms of dynamic response and harmonic suppression.

The behavior of a grid-connected PV system is extremely sensitive to the performance of the current control strategy in use. This research compares different control approaches, it starts with three controllers, which are Proportional-Integral (PI) controller, Proportional-Resonant (PR) controller and Fuzzy Logic Controller (FLC). Besides, an optimizations algorithm based on metaheuristics is used to optimize the FLC to enhance its adaptation capability and transient reaction to different environmental and loading conditions.

3.1. PI Controller

The PI controller is applied in the synchronous rotating dq-reference frame, where the three-phase AC signals are transformed into DC components. The controller regulates the current by adjusting the inverter output voltage to follow the reference current. Although the PI controller performs well in steady-state conditions, it struggles to track sinusoidal references directly in the stationary frame and is sensitive to parameter variations and harmonics [18], [19].

3.2. PR Controller

The PR controller is adopted in the stationary (αβ) frame and is implemented to provide high gain at a specific resonant frequency (typically the fundamental grid frequency) [20], [21], [22]. It enables direct tracking of sinusoidal signals without coordinate transformation. In general, the PR controller's transfer function is formulated as:

$$G_{PR} = K_P + K_I \frac{2\omega.s}{s^2 + 2\omega_c.s + \omega_0^2} \tag{1}$$

Where Kp and Kr are respectively the proportional and resonant gains, ω is the angular frequency of the grid. The PR controller offers better harmonic rejection but requires precise tuning. As illustrated in Figure 2, the resonant peak reaches a gain of 40 dB enabling efficient voltage tracking [20].

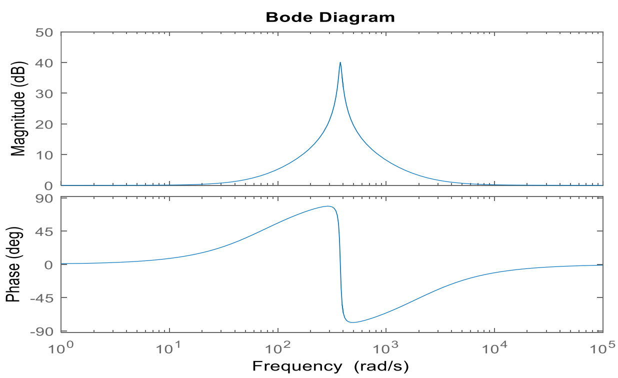

Figure 2. Frequency behavior of a non-ideal PR corrector with $K_P = 1$, $K_I = 100$, ωc=10 (rad/s)

Received: August 06 2025

International Journal of Applied Mathematics
Volume 38 No. 8s, 2025
ISSN: 1311-1728 (printed version); ISSN: 1314-8060 (on-line version)

3.3 Fuzzy Logic Controller (FLC)

The FLC is based on a rule strategy that use linguistic variables and inference rules to control the output [23], [24]. The inputs to the fuzzy controller are typically:

- Error e(t) (difference between reference and measured current)
- Change in error Δe(t)
- The output is a control signal (e.g., voltage or PWM modulation index) determined using a fuzzy inference system (FIS), which includes:
- Fuzzification
- Rule base (e.g., 7×7 or 5×5 rules) [25], [26]
- Inference engine
- Defuzzification

In this research, a PLL is employed to align the Park transformation with fluctuation in grid voltage fluctuations. Additionally, the FLC is applied to regulate both direct and quadrature currents control. Under steady-state conditions, the Park transformation amplitude V_d equals measured voltage amplitude and V_q retains a value of zero. The active power element characterized by I_d and the reactive power constituent characterized by I_q is given by equations (2) and (4) of [27], [28], [29]. The fuzzy logic regulator's block diagram that was applied in the undertaking of this research work is shown in the figure below.

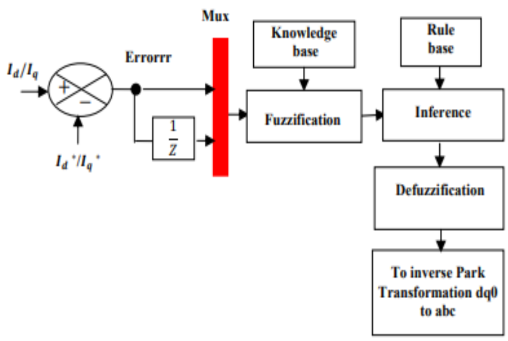

Figure 3. Schematic diagram of fuzzy logic corrector

Although the FLC effectively manages system nonlinearities and uncertainties, its performance is impacted by sensitive to the appropriate tuning of membership functions and rule sets.

4. Particle Swarm Optimization

4.1 Optimization of the FLC

In order to better the accuracy, adaptability and dynamic response of the FLC, a set of optimizations over the parameters of the FLC are implemented. In this study, the Particle Swarm Optimization (PSO) algorithm was chosen simply because of its simplicity, fast convergence and quality of coping with nonlinear search space [30], [31].

Received: August 06 2025

International Journal of Applied Mathematics
Volume 38 No. 8s, 2025
ISSN: 1311-1728 (printed version); ISSN: 1314-8060 (on-line version)

4.2 Objective

This paper sets out to optimize the internal parameters of a fuzzy logic controller (FLC) in a power electronic (PE)-based grid-connected photovoltaic (PV) system to enhance dynamic performance and power quality [32], [33]. A population-based metaheuristic algorithm defined as Particle Swarm Optimization (PSO) is used in performing automatic tuning of the FLC by adjusting:

- The positions of the input membership function (MFs),
- The normalization and de-normalization gains of the inputs and output.

4.3 Principle of PSO

PSO draws its cues from the swarming of birds or schooling of fish. It uses a set of solution candidates, termed a **particle** [34], that locally search the space based on their own experiences as well as the experiences of the entire swarm. Each particle updates its **velocity** and **position** according to the following equations:

The velocity and position updates follow these equations:

$$\mathbf{v_i(t+1)=v_i(t)+c_1 \cdot r_1 \cdot (p_i - x_i)+c_2 \cdot r_2 \cdot (g - x_i)} \quad (2)$$

$$\mathbf{x_i(t+1) = x_i(t)+v_i(t+1)} \quad (3)$$

Where :

- $x_i(t)$: Current position (solution) of particle i,
- $v_i(t)$: Current velocity,
- p_i : Particle's best known position,
- g : Global best position among all particles,
- r_1, r_2 : Random values in [0,1],
- ω, c_1, c_2 : Inertia weight, cognitive and social acceleration coefficients, respectively.

4.4 Parameters to Optimize

The fuzzy logic controller is composed of two input variables, "error e" and "change of error Δe" and one output variable that adjusts the modulation signal to the inverter. Each input is associated with three triangular membership functions (MFs). The positions of these MFs, along with normalization and de-normalization gains, are the parameters selected for optimization. Let the parameter vector be defined as:

$$\mathbf{x = [e_1, e_2, e_3, \Delta e_1, \Delta e_2, \Delta e_3, ke, k\Delta e, kout]} \quad (4)$$

Where:

Received: August 06 2025

- **e_i, Δ_{ei}** : MF centers for the inputs,
- **ke, kΔe** : Normalization gains for the inputs,
- **kout** : Gain applied to the defuzzified output.

4.5 Objective Function Definition

PSO is used to determine the optimal parameters of the membership functions and rule weights that minimize J. The results show that the optimized FLC outperforms other controllers under transient conditions, improving harmonic suppression and power quality.

The objective function is defined to minimize a composite performance index:

$$\mathbf{J = \omega 1 \cdot THD + \omega 2 \cdot TDD + \omega 3 \cdot (1 - Power\ Factor) + \omega 4 \cdot tr} \quad (5)$$

where:

- **THD** : Total Harmonic Distortion of the grid current,
- **TDD** : Total Demand Distortion,
- **PF** : Power factor measured at the grid interface,
- **tr** : Current response rise time,
- **ωi** : Weight coefficients chosen based on control objectives

The lower value of **J**, the better FLC's performance.

To accurately evaluate power quality in the studied three-phase system, several key performance indices are utilized: Total Harmonic Distortion (THD), Total Demand Distortion (TDD), and Power Factor (PF). These metrics are essential for quantifying waveform distortion and assessing the efficiency of power delivery under both linear and nonlinear load conditions.

Total Harmonic Distortion (THD) quantifies the harmonic content relative to the fundamental component. For current or voltage waveforms, it is defined as [35]:

$$THD\ (\%) = \frac{\sqrt{\sum_{n=2}^{\infty} X_n^2}}{X_1}.100 \quad (6)$$

Where Xn represents the RMS value of the n^{th} harmonic (either current In or voltage Vn), and X_1 is the RMS value of the fundamental component.

Total Demand Distortion (TDD) offers a load-normalized measure of harmonic distortion and is particularly relevant for current in three-phase power systems. It is given by [36]:

Received: August 06 2025

Volume 38 No. 8s, 2025
ISSN: 1311-1728 (printed version); ISSN: 1314-8060 (on-line version)

$$TDD\ (\%) = \frac{\sqrt{\sum_{n=2}^{\infty} I_n^2}}{I_L}.100 \tag{7}$$

Where I_L is the peak demand load current at rated conditions.

Power Factor (PF) is an indication of how good the system is at the conversion of electric power to useful work. It is described as [37]:

$$\text{PF} = \frac{P}{S} = \frac{P}{\sqrt{P^2 + Q^2}} \tag{8}$$

Where P is the active power, Q is the reactive power and S is the apparent power [37].

These formulas are used in this research on both the voltage and current waveforms taken out of the simulation results, and they allow making an extensive comparison of control strategies regarding harmonic distortion and efficiency of power delivery.

4.6 Flowchart of the Optimization Process

The following figure illustrates the optimization process from initialization to final FLC-PSO implementation:

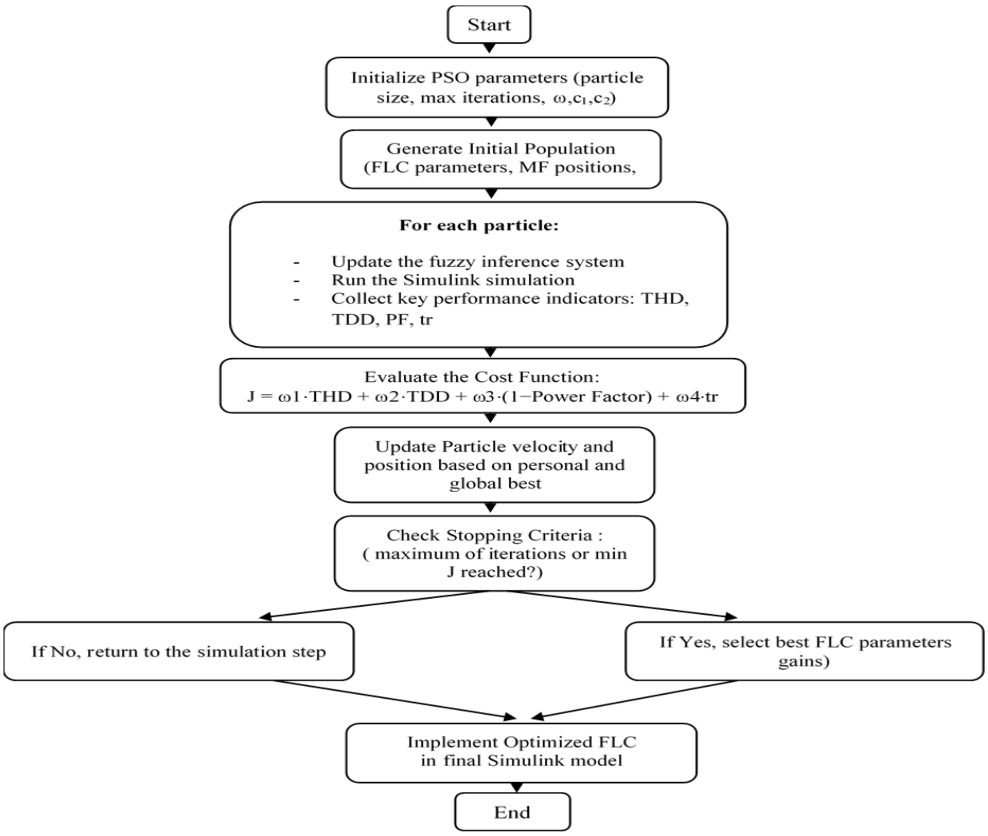

Figure 4. Optimization Process Flowchart

Received: August 06 2025

Volume 38 No. 8s, 2025
ISSN: 1311-1728 (printed version); ISSN: 1314-8060 (on-line version)

5. Simulation Results and Discussion

This section introduces and discusses the simulation results of the grid-connected PV-system under multiple operating scenarios. The aim is basically to compare the performance of various current control strategies, that is, PI, PR, and Fuzzy Logic Controllers (with and without PSO optimization), based on the basis of dynamic response, harmonic mitigation, and power quality. The nonlinear load conditions are also added to the simulation scenarios as well as the disturbances like an abrupt increase or decrease in irradiance and temperature. Their comparison is undertaken in terms of discriminating benchmarks of the main performance criteria, including total harmonic distortion (THD), transient response and accuracy of steady-state. The results give an idea about the effectiveness and resilience of every control strategy in the PV system.

The results discussed in this section are obtained from Matlab/Simulink simulations. As is shown in figure 5, the integrated system incorporates a PV module to generate a maximum output of 100 kW when the irradiance reaches 1000 W/m². Detailed parameters of the system investigated are presented in the appendix.

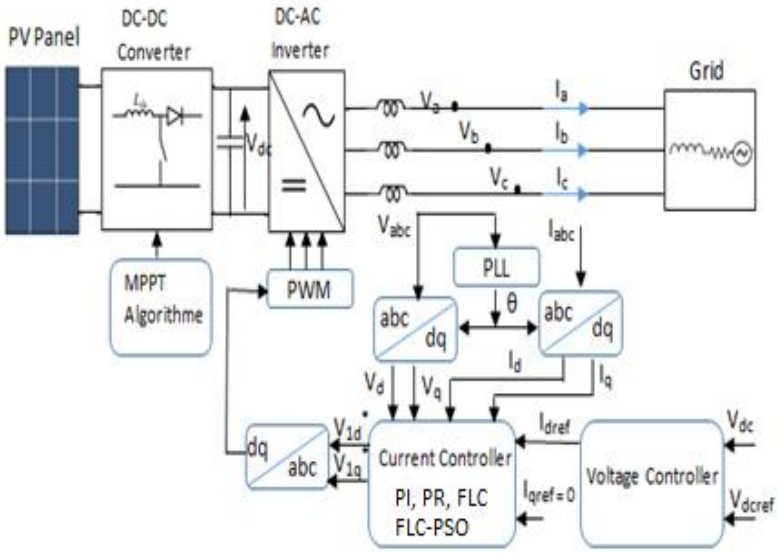

Figure 5. Detailed system modeling using MATLAB/Simulink

A. System Response Under Standard Test Conditions (STC)

In this initial scenario, the performance of the PV system is evaluated under Standard Test Conditions, which correspond to an irradiance of 1000 W/m² and a temperature of 25°C.

1. Active and reactive power under linear load variation

Figure 6 illustrates the transient behavior of active and reactive power when a nonlinear load is introduced at **t = 0.3 s**, with system operating under the control of PI, PR, FLC, and FLC-PSO regulators.

Received: August 06 2025

International Journal of Applied Mathematics

Volume 38 No. 8s, 2025

ISSN: 1311-1728 (printed version); ISSN: 1314-8060 (on-line version)

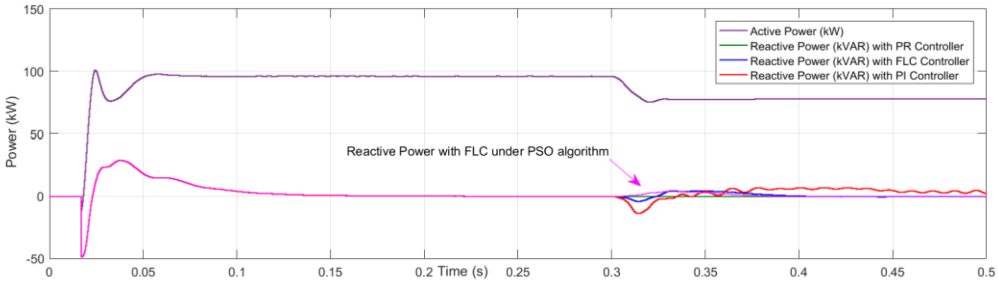

Figure 6. Active and reactive power controlled using different controller under addition of non-linear load

Each controller demonstrates unique characteristics in its response to this disturbance. The **PI controller** shows limitations in dealing with the sudden load change, as indicated by significant oscillations in reactive power. This unstable behavior reveals its limited ability to regulate power flow effectively during dynamic events and highlights its weakness in maintaining a consistent power factor. On the other hand, the **FLC controller** responds with greater flexibility. When the load is applied, the reactive power briefly spikes into the positive domain but quickly settles back to its nominal value. Despite slight oscillations throughout the settling process, the controller depicts significant progress in responding to disturbances as compared to the strategy of PI. The parameter optimization solution based on the PSO algorithm offers better performance. It also recovers quickly due to the perturbation, and it settles down with no observable overshoots or oscillations with improved dynamic response and stability of the system. The PR controller gives the most efficient response among the calculated strategies. It successfully stops the flow of reactive power, thus only injecting active power into the grid-even when the nonlinear load is impressed. This is characteristic of its ability to withstand power quality and efficiency in demanding load conditions. To draw up this conclusion, it can be noticed that both the FLC and FLC-PSO controllers can provide powerful control from disturbances. However, the PR controller has the highest capacity to reduce reactive power injection and maintain stability of the overall power system in grid-connected PV applications.

2. Current Overshoot Behavior under Nonlinear Load Conditions

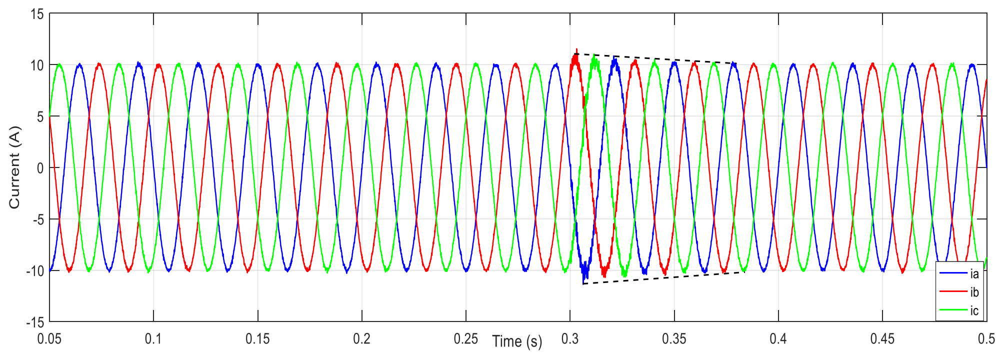

Received: August 06 2025

International Journal of Applied Mathematics
Volume 38 No. 8s, 2025
ISSN: 1311-1728 (printed version); ISSN: 1314-8060 (on-line version)

(a)

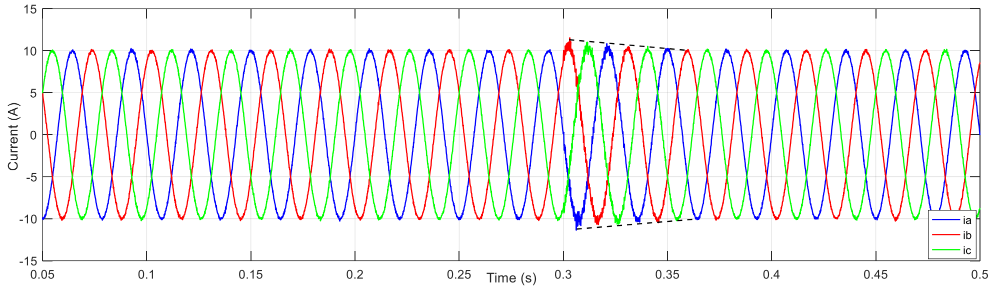

(b)

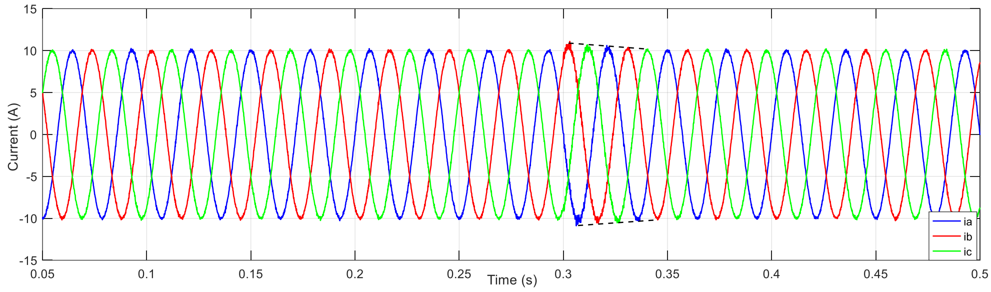

(c)

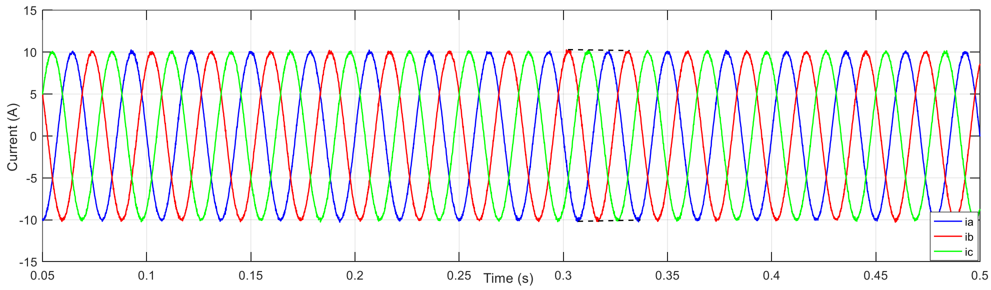

(d)

Figure 7. Three phase grid connected PV system with current overshoot, (a) PI, (b) PR, (c) FLC, (d) FLC- PS0

When a nonlinear load is connected to the studied system at time **t = 0.3s**, a sharp current overshoot is observed in **Figure 7** due to the sudden increase in harmonic content and dynamic current demand. This transient behavior challenges the controller's ability to regulate current and maintain power quality. Quantitatively, the PI controller exhibits the highest current overshoot, reaching approximately **14.1%**, and takes around **75.2 ms** to stabilize. The PR controller performs slightly better, reducing the overshoot to **13.9%** with a shorter settling time of **56.7 ms**. The fuzzy logic controller (FLC) shows a more robust response, limiting the overshoot to **9.57%** and stabilizing at **37.4 ms**. The most effective performance is achieved with the optimized FLC using the PSO algorithm (FLC-PSO), which limits the current overshoot to only **3.64%** and achieves full stabilization in less than **27.8**

Received: August 06 2025

International Journal of Applied Mathematics

Volume 38 No. 8s, 2025

ISSN: 1311-1728 (printed version); ISSN: 1314-8060 (on-line version)

ms. These results demonstrate the significant impact of advanced and optimized control strategies on mitigating transient disturbances, particularly in the presence of nonlinear loads.

3. FFT-Based Harmonic Analysis

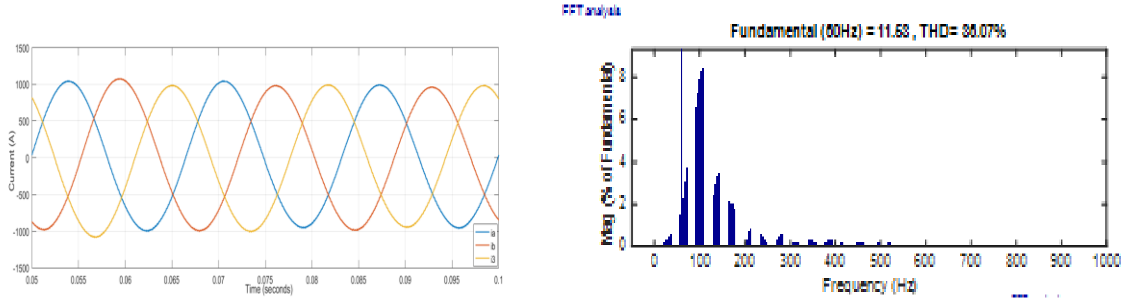

(a)

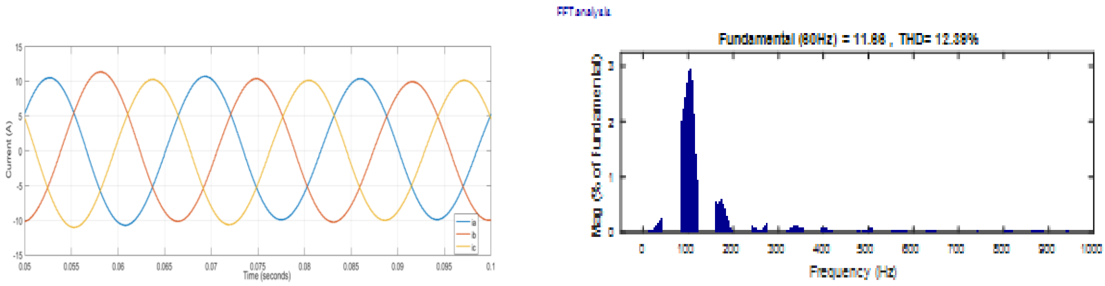

(b)

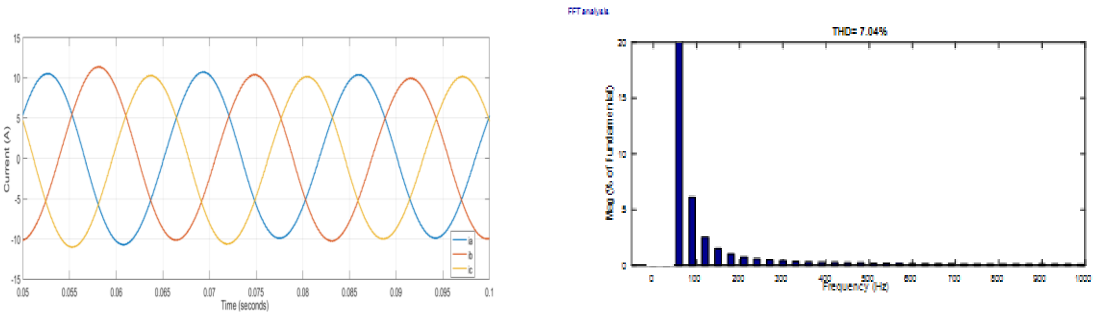

(c)

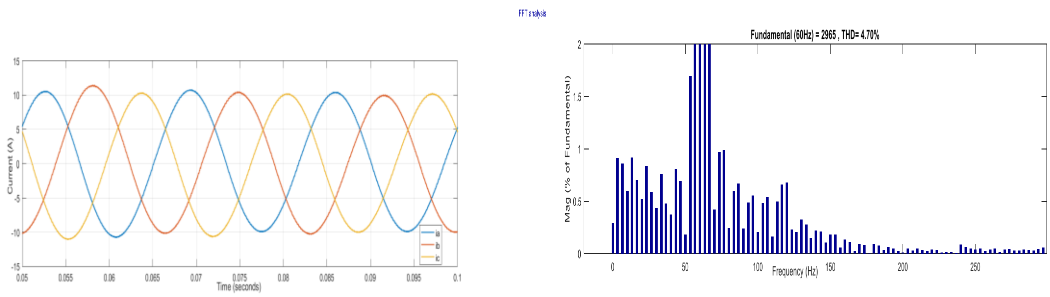

(d)

Figure 8. Grid-Connected current waveform and corresponding harmonic characteristics & THD : (a) PI, (b) PR, (c) FLC, (d) FLC-PSO

Received: August 06 2025

International Journal of Applied Mathematics

Volume 38 No. 8s, 2025

ISSN: 1311-1728 (printed version); ISSN: 1314-8060 (on-line version)

Figure 8 illustrates the spectral content of the grid-injected current and the corresponding THD values when supplying a nonlinear load, under the control of different types of regulators. The simulation results clearly demonstrate that the Fuzzy Logic Controller optimized by Particle Swarm Optimization (FLC-PSO) achieves the lowest Total Harmonic Distortion among all tested controllers (**4.7 %**). Compared to conventional FLC (**7.04 %**), PR (**12.39 %**), and PI strategies (**36.07 %**), the FLC-PSO exhibits a noticeable improvement in harmonic suppression, confirming its superior performance in maintaining current quality under distorted loading conditions.

4. Steady-State Error and Current Tracking Performance

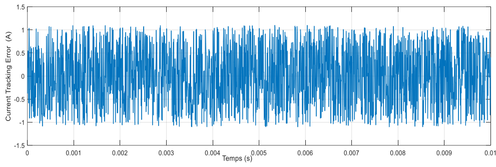

(a)

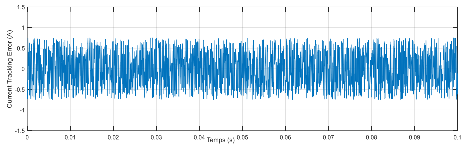

(b)

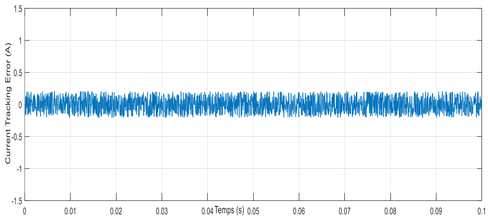

(c)

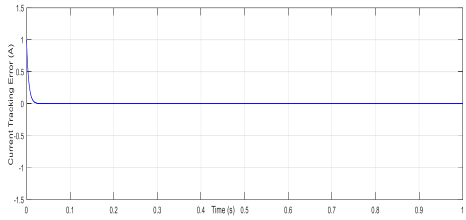

(d)

Figure 9. Current Tracking Error

The PI controller presents a steady-state current error oscillating within **±1.0 A**, which reflects limited stability and significant current fluctuations. Similarly, the PR controller shows a broad error margin, though slightly improved, constrained to **±0.72 A**. With the Fuzzy Logic Controller (FLC), the steady-state error is reduced to **±0.18 A**, yet still indicates suboptimal stability. In contrast, the FLC, enhanced by Particle Swarm Optimization (FLC-PSO), demonstrates superior regulation, maintaining steady-state error within a narrow range of **±0.04 A**. This controller not only minimizes current ripple but also provides faster response and more accurate current tracking, ensuring effective synchronization with the grid.

5. Voltage Performance

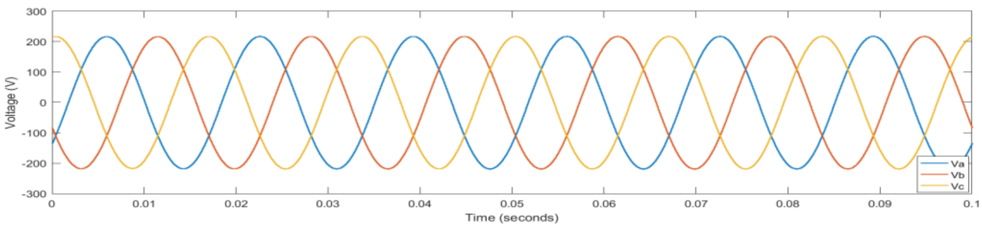

Figure 10. Voltage waveform at V_{PCC}

Received: August 06 2025

Volume 38 No. 8s, 2025
ISSN: 1311-1728 (printed version); ISSN: 1314-8060 (on-line version)

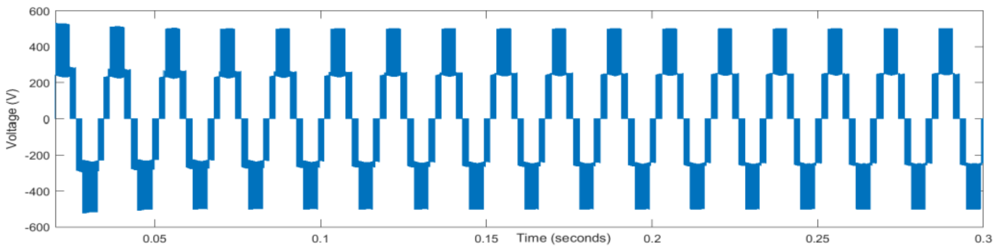

Figure 11. Inverter output line voltage

Figure 10 illustrates the voltage waveform at the V_{PCC} over the time interval from 0 to 0.1s. The waveform maintains a consistent amplitude of 220 V with a stable and balanced shape, showing a 120° phase shift between each phase. As shown in the same figure, the inverter's line voltage output reaches 500 V during this period, which corresponds to the DC-side voltage V_{dc}, also observable in Figure 11.

6. Dynamic Response and Transient Performance

The table and the diagram below summarize the different parameter values obtained by the harmonic analysis:

Table 1. Summary table comparing parameters results

	PI	**PR**	**FLC**	**FLC-PSO**
TDD (%)	49.85	20.7	12.75	**8.20**
THD (%)	36.07	12.39	7.04	**4.7**
PF	0.86	0.92	0.97	**0.98**
Dynamic Response	Slow	Faster	Good	**Best**

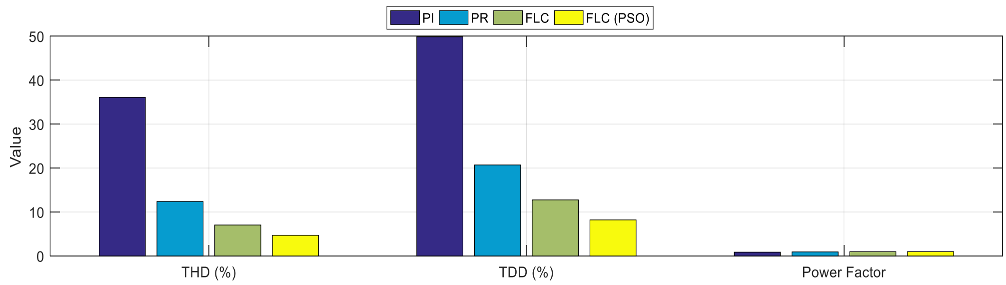

Figure 12. Diagram comparing parameters results

– The TDD is significantly reduced when using FLC, and even further with FLC-PSO. The PI controller performs poorly, with TDD more than 6× higher than the best solution,

– Again, FLC-PSO outperforms all others, with a very low THD compared to the other controllers,

– High PF indicates better efficiency. , FLC and FLC-PSO achieve high power factor, showing better reactive power compensation,

Received: August 06 2025

Volume 38 No. 8s, 2025
ISSN: 1311-1728 (printed version); ISSN: 1314-8060 (on-line version)

– FLC-PSO achieves the best transient behavior, confirming it as the most responsive and stable controller.

From all these facts, the FLC-PSO controller maintains the TDD well below the 8% threshold typically enforced for nonlinear loads, ensuring that the system satisfies both utility requirements and power quality standards.

B. System Response Under Variable Test Conditions

To evaluate the robustness of the control strategies under realistic operating scenarios, the system was subjected to varying irradiance and temperature profiles, simulating fluctuating weather conditions. These changes introduce dynamic disturbances that directly impact the PV array's output and challenge the controllers' ability to maintain stable grid injection. The dynamic behavior of the proposed control strategies was further assessed under three distinct environmental scenarios: **step-wise irradiance variation (Case 1)**, **temperature fluctuations (Case 2)**, and **real-time irradiance conditions (Case 3)**.

Case 1: Changing Irradiance Conditions

In **Case 1 (Figure 13 (a))**, where irradiance levels were varied in discrete steps while maintaining a constant temperature (25 °C), the **FLC-PSO controller** delivered the most consistent and accurate power output. **Figure 13(b)**, shows that the PV output tracked the irradiance profile with minimal delay and very low overshoot, indicating the effectiveness of PSO optimization in enhancing fuzzy logic rule tuning. In contrast, the **PI and PR controllers** exhibited delayed responses and power oscillations during irradiance transitions, confirming their reduced adaptability in the face of abrupt solar changes. The standard **FLC controller** performed reasonably well but still showed minor deviations in power tracking, particularly during downward irradiance steps.

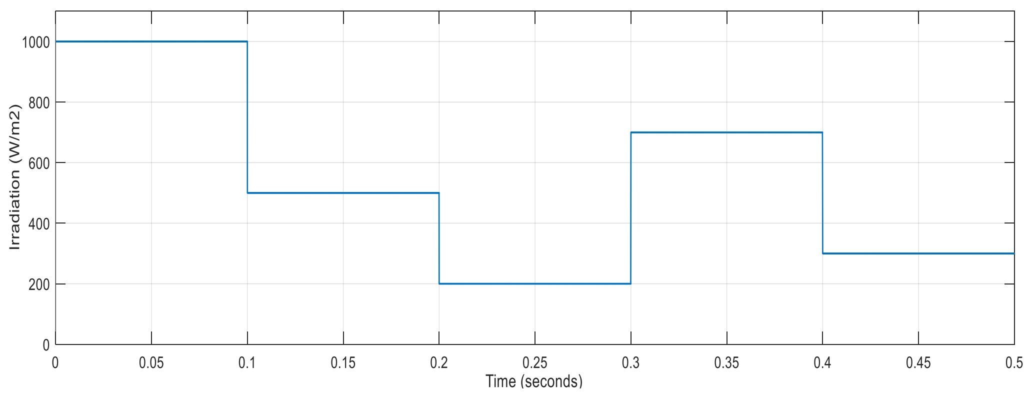

(a)

Received: August 06 2025

International Journal of Applied Mathematics

Volume 38 No. 8s, 2025

ISSN: 1311-1728 (printed version); ISSN: 1314-8060 (on-line version)

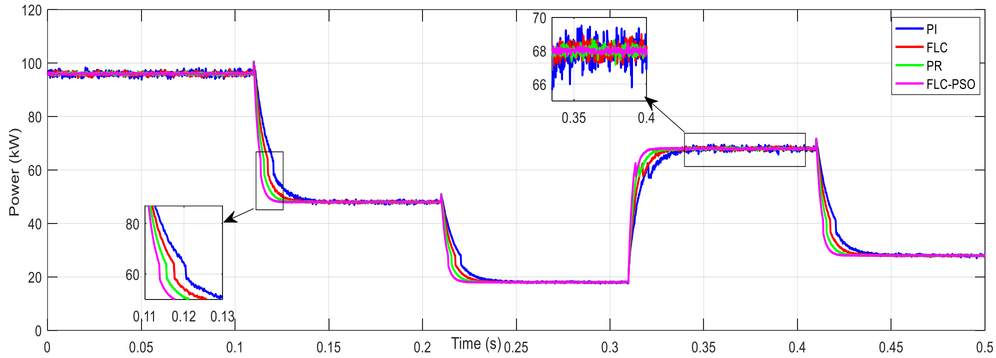

(b)

Figure 13. System response under changing irradiance conditions: (a) Changing irradiance profile, (b) PV output power under different control methods

Case 2: Changing Temperature Conditions

In **Case 2 (Figure 14 (a))**, with constant irradiance and varying temperature, thermal disturbances introduced additional nonlinearity in the PV output. Again, the **FLC-PSO controller** demonstrated superior thermal robustness, quickly compensating for the changing PV characteristics. In **figure 14 (b)**, the **FLC** controller also showed resilience but required slightly more time to stabilize. Both PI and PR controllers were more sensitive to temperature fluctuations, resulting in slower adaptation and noticeable ripples in the output power.

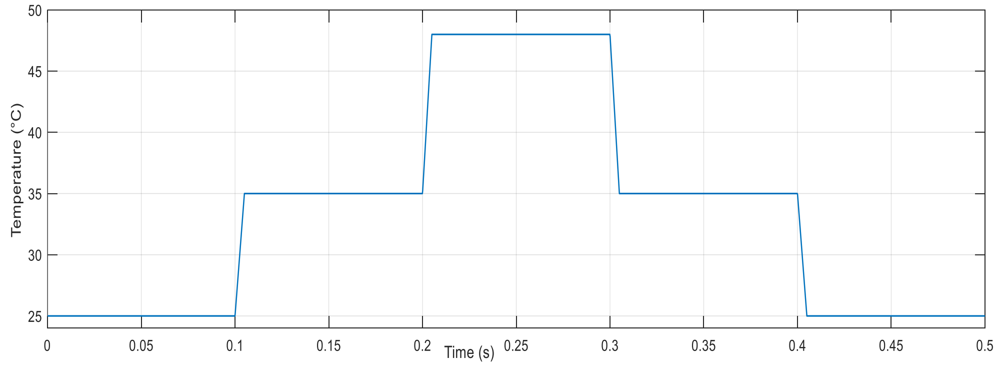

(a)

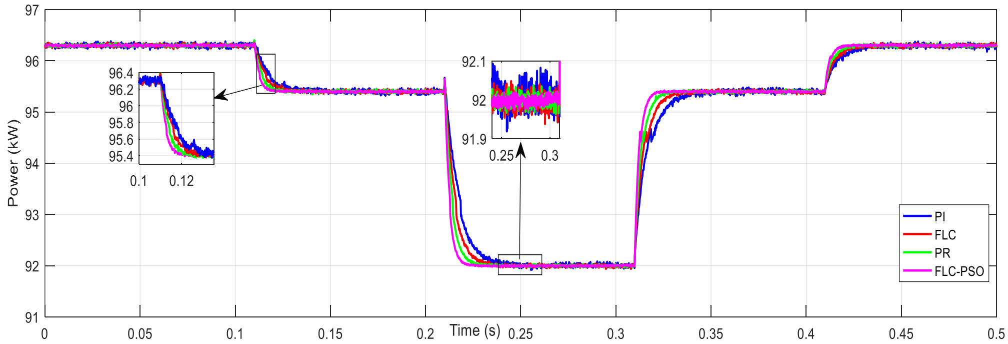

(b)

Received: August 06 2025

International Journal of Applied Mathematics

Volume 38 No. 8s, 2025

ISSN: 1311-1728 (printed version); ISSN: 1314-8060 (on-line version)

Figure 14. System response under changing irradiance conditions: (a) Changing temperature profile, (b) PV output power under different control methods

Case 3: Real Time Irradiance Conditions

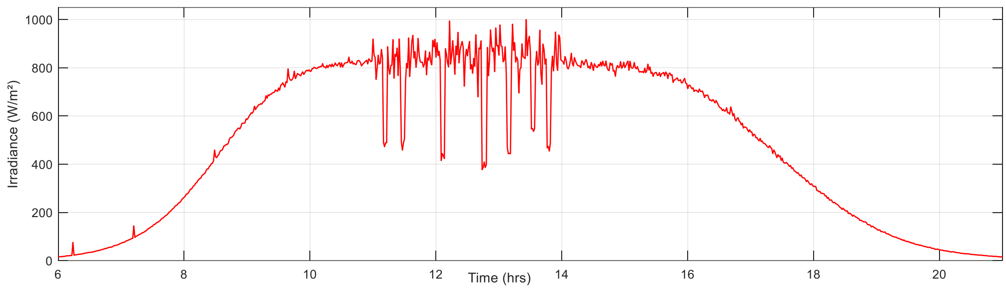

(a)

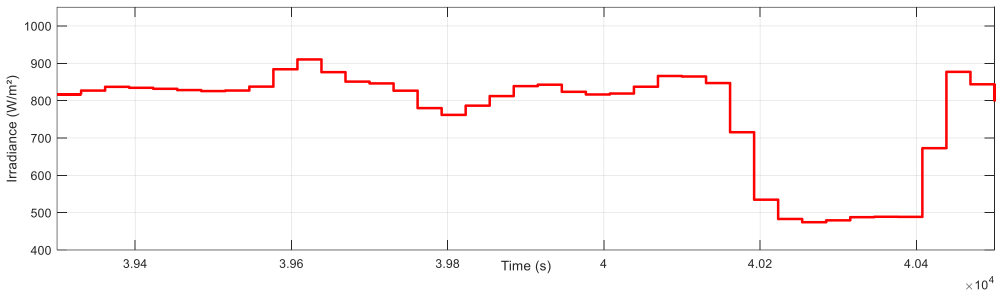

(b)

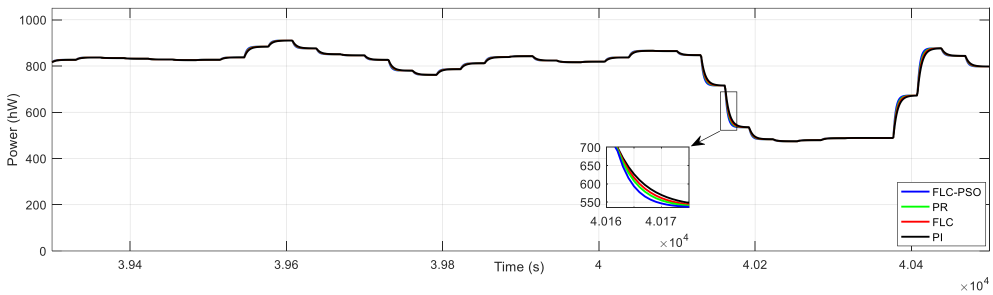

(c)

Figure 15. System response under real time irradiance condition: (a) Real time irradiance (b) Samples of irradiance (c) PV output power under different control methods

The performance of the proposed method under rapidly changing irradiance and constant temperature (25 °C) is studied using real-time data samples.

The real-time data was gathered similar to that of a weather station. **Figure 15(a)** shows the rapid changes in the irradiance on a particular day from 6am to 10pm. In order to simulate abruptly changing irradiance, some data samples of irradiance are collected at regular intervals from 10:50 AM to 11:20 AM. The collected data is given as a step input, and it is considered that the changes occur every 0.1 s as shown in **Figure 15(b)**.

Received: August 06 2025

Volume 38 No. 8s, 2025
ISSN: 1311-1728 (printed version); ISSN: 1314-8060 (on-line version)

In **Figure 15(c)**, it can be seen clearly that the **FLC-PSO controller** maintained smooth and stable power delivery throughout the real-time irradiance fluctuations, effectively filtering out noise and handling transient dips. The **PR** and **FLC** controllers followed the trend moderately well, though with reduced precision in low-irradiance periods. The **PI controller**, however, struggled with both response speed and stability, especially when irradiance rapidly declined. These results emphasize the significant advantage of combining fuzzy logic with evolutionary optimization techniques such as PSO to handle the nonlinear and unpredictable nature of environmental variations in PV systems. The **FLC-PSO strategy consistently delivers high-quality, reliable power output**, positioning it as a robust solution for grid-connected PV applications under varying real-world conditions.

6. Conclusion

This study has provided a comprehensive evaluation of different current control strategies—namely PI, PR, FLC, and PSO-optimized FLC—in a grid-connected photovoltaic (PV) system supplying nonlinear loads under both standard and dynamic environmental conditions. The simulation results clearly highlight the limitations of traditional linear controllers, particularly the PI controller, which suffered from high harmonic distortion, significant current overshoot (up to 14.1%), and slower response times.

The PR controller demonstrated improved dynamic behavior and reduced THD and TDD compared to the PI regulator, but it remained sensitive to changes in temperature and irradiance. The standard fuzzy logic controller showed stronger adaptability and robustness, especially in mitigating transient effects and enhancing steady-state performance.

The most notable outcome of this research lies in the deployment of the **FLC optimized by Particle Swarm Optimization (FLC-PSO)**. This intelligent control technique outperformed all other strategies, achieving:

- The **lowest THD (4.7%)** and **TDD (8.2%)**, below IEEE 519 standards,
- The **highest power factor (0.98)** even under nonlinear loading,
- The **shortest current settling time (27.8 ms)** and **minimal overshoot (3.64%)**,
- Superior performance in real-time irradiance and temperature variations.

These results confirm that combining fuzzy control with metaheuristic optimization offers an efficient and intelligent solution for improving the power quality of PV systems in real-world conditions.

Future work may extend this research to real-time experimental validation, integration with hybrid renewable energy systems, or the application of advanced evolutionary algorithms to further strengthen control adaptability and resilience.

Appendix

Appendix A: Photovoltaic panel specification

Received: August 06 2025

Volume 38 No. 8s, 2025

ISSN: 1311-1728 (printed version); ISSN: 1314-8060 (on-line version)

Temperature	**T**	**25**	**°C**
Open circuit voltage	V_{oc}	**64.2**	**V**
Short circuit current	I_{sc}	**5.96**	**A**
Voltage maximum power	V_{max}	**54.7**	**V**
Current maximum power	I_{max}	**5.58**	**A**
Maximum power	P_{max}	**305**	**W**

Appendix B: PV system connected to grid parameters

Irradiance	**1000 W/m**
Temperature	**25 °C**
Output power *P*	**100 kW**
MPPT Controller	**P&O**
DC side voltage V_{DC}	**273.5 V**
DC side voltage reference	**500 V**
AC side voltage V_{AC}	**260 V**
Transformer voltage levels	**260V/25kV**
Apparent power	**100 kVA**
Distribution feeders	**25 kV**
Equivalent transmission networks	**120 kV**

References

[1] V. Khanna, B. K. Das, and D. Bisht, "Matlab/simelectronics models based study of solar cells," *Int. J. Renew. Energy Res.*, vol. 3, no. 1, pp. 30–34, 2013.

[2] H. Ouatman, "Modeling and Control of a Grid-Connected PV Energy Conversion System," vol. 10, pp. 484–492, 2015.

Received: August 06 2025

ISSN: 1311-1728 (printed version); ISSN: 1314-8060 (on-line version)

[3] M. D. M. Wail Rezgui, Leila Hayet Mouss, "Modeling of a photovoltaic field in malfunctioning," in *International Conference on Control, Decision and Information Technologies (CoDIT)*, p. 2013.

[4] P. K. S. A.H. Mollah, G.K.Panda, "Three Phase Grid Connected Photovoltaic System with Maximum Power Point Tracking," *Int. J. Adv. Res. Electr. Electron. Instrum. Eng.*, vol. 4, no. 5, p. ISSN (Online): 2278 – 8875.

[5] H.-S. N. Tsai-Fu Wu and S. Chih-Lung, "A single-phase inverter system for PV power injection and active power filtering with nonlinear inductor consideration," in *IEEE Transactions on Industry Applications*, 2005.

[6] S. E. B, T. Khalili, and M. Oulcaid, "Impact Study of Harmonic Analysis of a Grid-Connected Photovoltaic System Feeding Nonlinear Load," vol. 1, pp. 18–29.

[7] Z. Yao and L. Xiao, "Control of single-phase grid-connected inverters with nonlinear loads," *IEEE Trans. Ind. Electron.*, vol. 60, no. 4, pp. 1384–1389, 2013, doi: 10.1109/TIE.2011.2174535.

[8] S. M. A. Sayal, P.C. Sekhar, "A Review on Maximum Power Point Tracking Techniques for Photovoltaic Power Generating Systems," in *National Electrical Engineering Conference (NEEC-2011) on Power and Energy Systems for Tomorrow*, 2011.

[9] T. Laagoubi, M. Bouzi, and M. Benchagra, "Analysis and comparison of MPPT nonlinear controllers for PV system," *Proc. 2015 IEEE Int. Renew. Sustain. Energy Conf. IRSEC 2015*, no. November 2016, 2016, doi: 10.1109/IRSEC.2015.7455012.

[10] S. Ozdemir, "Z-source T-type inverter for renewable energy systems with proportional resonant controller," *Int. J. Hydrogen Energy*, vol. 41, no. 29, pp. 12591–12602, Aug. 2016, doi: 10.1016/J.IJHYDENE.2016.01.140.

[11] C. ZELICI, "A THREE THRE E - PHASE PWM INVERTER WITH W ITH," 2012.

[12] Abd Almula G. M. Gebreel, "Simulation and Implementation of Two- Level and Three-Level Inverters By Matlab and Rt-Lab," *MSc Thesis*, p. 155, 2011.

[13] I. Alhamrouni, M. A. Hairullah, N. S. Omar, M. Salem, A. Jusoh, and T. Sutikno, "Modelling and design of PID controller for voltage control of AC hybrid micro-grid," *Int. J. Power Electron. Drive Syst.*, vol. 10, no. 1, p. 151, 2019, doi: 10.11591/ijpeds.v10.i1.pp151-159.

[14] G. C. R. Kadri, J. Gaubert, "An Improved maximum power point tracking for photovoltaic grid-connected inverter based on voltage-oriented control," *IEEE Trans. Ind. Electron.*, vol. 58, no. 1, pp. 66–75, 2011, doi: 10.1109/TIE.2010.2044733.

[15] H. Cha, T. K. Vu, and J. E. Kim, "Design and control of proportional-resonant controller based Photovoltaic power conditioning system," *2009 IEEE Energy Convers. Congr. Expo. ECCE 2009*, pp. 2198–2205, 2009, doi: 10.1109/ECCE.2009.5316374.

Received: August 06 2025

Volume 38 No. 8s, 2025
ISSN: 1311-1728 (printed version); ISSN: 1314-8060 (on-line version)

[16] D. K. P. S.Mari devi1, "RESONANT CURRENT CONTROLLER BASED THD REDUCTION IN AC MICRO," *Eng. Electron. Eng. Electron.*, vol. 22, no. 2, pp. 425–429, 2016.

[17] M. CHEBRE, M. ZERIKAT, and Y. BENDAHA, "Adaptation des Paramètres d ' un Contrôleur PI par un FLC Appliqué à un Moteur Asynchrone," in *4th International Conference on Computer Integrated Manufacturing CIP'2007*, 2007, no. November, pp. 2–7.

[18] L. K. Letting, J. L. Munda, and Y. Hamam, "Optimization of a fuzzy logic controller for PV grid inverter control using S-function based PSO," *Sol. Energy*, vol. 86, no. 6, pp. 1689–1700, 2012, doi: 10.1016/j.solener.2012.03.018.

[19] M. S. Omar, A. L. E. S. Amgad El-Deib, and and M. E. A. M. A. El.rhman, "Comparative Study Between PI and Fuzzy-Logic Controllers for Three-Phase Grid-Connected Photovoltaic Systems Photovoltaic Systems," *Proc. IEEE*, vol. 81, no. 3, pp. 365–377, 1993, doi: 10.1109/5.241491.

[20] S. Essaghir, M. Benchagra, and N. El Barbri, "Power factor control of a photovoltaic system connected to grid under load variation," in *Proceedings of 2017 International Conference on Electrical and Information Technologies, ICEIT 2017*, Jan. 2018, vol. 2018-Janua, pp. 1–7, doi: 10.1109/EITech.2017.8255285.

[21] S. Essaghir, M. Benchagra, and N. El Barbri, *Comparative Study of Three Phase Grid Connected Photovoltaic System Using PI, PR and Fuzzy Logic PI Controller with Harmonic Analysis*, vol. 624 LNEE. 2020.

[22] M. H. Ibrahim, S. P. Ang, and M. N. Dani, "Optimizing Step-Size of Perturb & Observe and Incremental Conductance MPPT Techniques Using PSO for Grid-Tied PV System," no. February, 2023.

[23] H. Hwang *et al.*, "Engineering Science and Technology , an International Journal Enhancing performance of shipboard photovoltaic grid-connected inverter through CRNN-LM-BP control optimized by particle swarm optimization of LCL parameters," vol. 57, no. May, 2024.

[24] V. K. Kamboj, "A novel hybrid PSO – GWO approach for unit commitment problem," *Neural Comput. Appl.*, 2015, doi: 10.1007/s00521-015-1962-4.

[25] N. G. E. L. Sayed, A. M. Yousef, G. El-saady, M. D. Alanazi, and H. A. Ziedan, "Eectrical grid linked to PV / wind system based fuzzy controller and PID controller tuned by PSO for improving LVRT," pp. 1–24, 2025.

[26] H. M. H. Farh, A. M. Eltamaly, and M. F. Othman, "Hybrid PSO-FLC for dynamic global peak extraction of the partially shaded photovoltaic system," pp. 1–16, 2018.

[27] S. A. Zaid and A. M. Kassem, "Review , analysis and improving the utilization factor of a PV-grid connected system via HERIC transformerless approach," vol. 73, no. February, pp. 1061–1069, 2017.

Received: August 06 2025

International Journal of Applied Mathematics

Volume 38 No. 8s, 2025

ISSN: 1311-1728 (printed version); ISSN: 1314-8060 (on-line version)

[28] P. Titulaire, "´ CHEIKH ANTA DIOP DE DAKAR UNIVERSIT E Ecole Doctorale : Physique , Chimie , Sciences de la Terre , de l ' Univers et de l ' Ing ´ enieur (ED-PCSTUI) Conception et commande de convertisseurs statiques pour moulins ` a moteurs asynchrones triphas ´ es," 2017.

Received: August 06 2025